The 1-(Trimethylsilyl)bicyclobutonium Ion: NMR Spectroscopy, Isotope Effects, and Quantum Chemical Ab Initio Calculations of a New Hypercoordinated Carbocation

Hans-Ullrich Siehl,*,†,‡ Martin Fuss,† and Jürgen Gauss§

Contribution from the Institut für Organische Chemie der Universität Tübingen, D-72076 Tübingen, Germany, Institute for Fundamental Research of Organic Chemistry, Kyushu University, Fukuoka, 813 Japan, and Lehrstuhl für Theoretische Chemie, Institut für Physikalische Chemie, Universität Karlsruhe, D-76128 Karlsruhe, Germany

Received February 24, 1995[⊗]

Abstract: The 1-(trimethylsilyl)bicyclobutonium ion is generated from (1′-(trimethylsilyl)cyclopropyl)methanol by reaction with SbF_5. The NMR spectroscopic data in SO_2ClF/SO_2F_2 solution at −128 °C are in accord with a bridged puckered bicyclobutonium structure undergoing a 3-fold rapid degenerate rearrangement that renders the two β- and one γ-methylene groups equivalent, leading to one averaged ^{13}C-NMR signal for the CH_2 groups at 48.9 ppm. Conformational ring inversion is slow so that two separate signals for the three averaged *endo*-CH_2 (4.04 ppm) and three averaged *exo*-CH_2 hydrogens (3.24 ppm) are observed. The deuterium equilibrium isotope effects for *exo*- and *endo*-CHD-labeled cations are different in sign and magnitude and are rationalized by different *endo*- and *exo*-C−H bond force constants at the pentacoordinated carbon. NMR chemical shift calculations for the 1-silylbicyclobutonium ion and the (1′-silylcyclopropyl)methyl cation were performed with the GIAO-SCF and GIAO-MP2 methods. The experimental shifts are satisfactorily reproduced by GIAO-MP2//tzp/dz calculated shifts for the 1-silylbicyclobutonium structure. The good agreement between theory and experiment supports a fully degenerate set of interconverting 1-(trimethylsilyl)bicyclobutonium ions and excludes contributions from other isomers to the observed equilibrium process. The geometric and electronic properties of the 1-(trimethylsilyl)bicyclobutonium cation are intermediate between those of the parent bicyclobutonium ion and those of the methyl-substituted analogue.

The cyclobutyl/cyclopropylmethyl cation system has been of continuing interest for many years.[1] On the basis of NMR spectroscopic investigations,[2] isotope effect experiments,[3] and quantum chemical calculations of geometry, chemical shifts, and vibrational frequencies,[4] the parent system $[C_4H_7]^+$ [5] is now best described as a degenerate set of rapidly interconverting bicyclobutonium ions (**1**) with minor contributions from another degenerate set of rapidly equilibrating cyclopropylmethyl cations which are only marginally higher in energy than **1** (<1 kcal mol^{-1}). For the analogous 1-methyl-substituted cation $[C_4H_6CH_3]^+$,[6] the investigations of equilibrium isotope effects on the NMR spectra of mono-[7] and dideuterated cations[8,9] and quantum chemical ab initio calculations[10] agree that this cation system can be adequately described by considering only one degenerate set of hypercoordinated puckered methylbicyclobutoniumion structures (**2**) without contributions from (1′-methylcyclopropyl)-methyl cation structures. In contrast, the isotope effects observed for the corresponding trideuterio-substituted cation have been interpreted by invoking the presence of a minor species in equilibrium with the major isomer.[11] The nature of the postulated minor species, however, is not clear.[1]

A trimethylsilyl group in the α-position to the positive charge in carbocations is destabilizing compared to an α-methyl group but has a stabilizing effect compared to an α-hydrogen.[12,13] This has been shown by Apeloig and Stanger on the basis of solvolytic studies and quantum chemical calculations[14] and has recently been confirmed by NMR spectroscopic investigations of α-silyl-substituted benzyl cations in solution.[15]

† Universität Tübingen.
‡ Kyushu University.
§ Universität Karlsruhe.
⊗ Abstract published in *Advance ACS Abstracts*, May 15, 1995.

(1) For recent reviews, see: (a) Olah, G. A.; Reddy, V. P.; Prakash, G. K. S. *Chem. Rev.* **1992**, *92*, 69. (b) Lenoir, D.; Siehl, H.-U. In *Houben-Weyl Methoden der Organischen Chemie*; Hanack, M., Ed.; Thieme: Stuttgart, Germany, 1990; Vol. E19c, p 413. (c) Olah, G. A.; Prakash, G. K. S.; Sommer, J. In *Superacids*; Wiley: New York, 1985; p 143. (d) In accord with our earlier work (refs 3, 7, 9, and 28), we use solid lines in all formulas to symbolize the connectivity and coordination of the atoms and not necessarily the nature of the bonding.

(2) (a) Staral, J. S.; Yavari, I.; Roberts, J. D.; Prakash, G. K. S.; Donovan, D. J.; Olah, G. A. *J. Am. Chem. Soc.* **1978**, *100*, 8016. (b) Yannoni, C. S.; Myhre, P. C.; Webb, G. G. *J. Am Chem. Soc.* **1990**, *112*, 8992.

(3) Saunders, M.; Siehl, H.-U. *J. Am. Chem. Soc.* **1980**, *102*, 6868.

(4) (a) Koch, W.; Liu, B.; DeFrees, D. J. *J. Am. Chem. Soc.* **1988**, *110*, 7325. (b) McKee, M. L. *J. Phys. Chem.* **1986**, *90*, 4908. (c) Saunders, M.; Laidig, K. E.; Wiberg, K. B.; Schleyer, P. v. R. *J. Am. Chem. Soc.* **1988**, *110*, 7652. (d) Vančik, H.; Gabelica, V.; Sunko, D. E.; Buzek, P.; Schleyer, P. v. R. *J. Phys. Org. Chem.* **1993**, *6*, 427.

(5) Olah, G. A.; Kelly, D. P.; Jeuell, C. L.; Porter, R. D. *J. Am. Chem. Soc.* **1970**, *92*, 2544.

(6) (a) Saunders, M.; Rosenfeld, J. *J. Am. Chem. Soc.* **1970**, *92*, 2548. (b) Olah, G. A.; Jeuell, C. L.; Kelly, D. P.; Porter, A. D. *J. Am. Chem. Soc.* **1972**, *94*, 146. (c) Olah, G. A.; Spear, R. J.; Hiberty, P. C.; Hehre, W. J. *J. Am. Chem. Soc.* **1976**, *98*, 7470. (d) Kirchen, R. P.; Sørensen, T. S. *J. Am. Chem. Soc.* **1977**, *99*, 6687. (e) Olah, G. A.; Prakash, G. K. S.; Donovan, D. J.; Yavari, J. *J. Am. Chem. Soc.* **1978**, *100*, 7085.

(7) Siehl, H.-U. *J. Am. Chem. Soc.* **1985**, *107*, 3390.

(8) Prakash, G. K. S.; Arvanaghi, M.; Olah, G. A. *J. Am. Chem. Soc.* **1985**, *107*, 6017.

(9) Siehl, H.-U. In *Physical Organic Chemistry 1986*; Kobayashi, M., Ed.; Elsevier: Amsterdam, 1987; p 25.

(10) (a) Schleyer, P. v. R.; Gauss, J.; Buzek, P. Private communication. (b) Buzek, P. Ph.D. Thesis, University of Erlangen, 1993.

(11) Saunders, M.; Krause, N.; *J. Am. Chem. Soc.* **1988**, *110*, 8050.

(12) (a) In *The chemistry of organic silicon compounds*; Patai, S., Rappoport, Z., Eds.; Wiley: New York, 1989; Chapter 2, p 193. (b) A recent review: Lambert, J. B. *Tetrahedron* **1990**, *46*, 2677. For the effect of an α-silyl group in carbanions and radicals, see: Zhang, S.; Zhang, X.-M.; Bordwell, F. G. *J. Am. Chem. Soc.* **1995**, 117, 602.

(13) Bausch, M. J.; Gong, Y. *J. Am. Chem. Soc.* **1994**, *116*, 5963.

(14) (a) Apeloig, Y.; Stanger, A. *J. Am. Chem. Soc.* **1985**, *107*, 2806. (b) Stang, P. J.; Ladika, M.; Apeloig, Y.; Stanger, A.; Schiavelli, M. D.; Hughey, M. R. *J. Am. Chem. Soc.* **1982**, *104*, 6852.

(15) Kaufmann, F.-P. Ph.D. Thesis, University of Tübingen, 1992.

0002-7863/95/1517-5983$09.00/0

We therefore perceived that the 1-trimethylsilyl-substituted cyclobutyl cation $[C_4H_6SiMe_3]^+$ (**3**) should have a bicyclobutonium structure similar to **1** and **2**. Since cation **3** might serve as a possible link between the structural and dynamical features of cations **1** and **2**, it represents an interesting target for experimental and concomitant computational studies. The cation **3** might undergo facile degenerate rearrangements equilibrating the methylene carbons on a flat potential energy surface as it has been observed for **1** and **2**. A conformational inversion process interchanging the geminal methylene protons which has been observed for the methyl bicyclobutonium ion **2** but not for the parent bicyclobutonium ion **1** is in principle also conceivable for cation **3**.

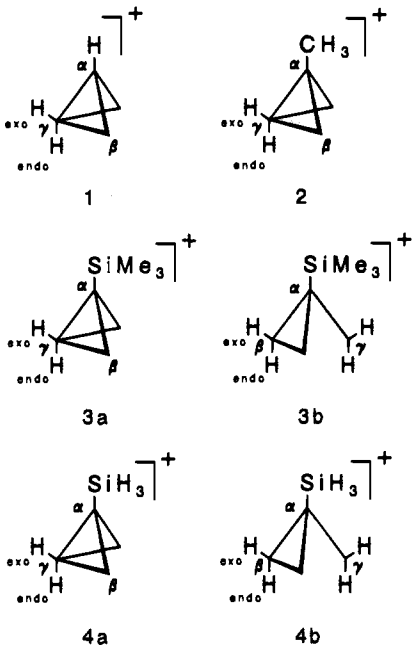

1 2 3a 3b 4a 4b

Results and Discussion

The cation **3** was generated by reaction of (1′-(trimethylsilyl)-cyclopropyl)methanol (**5**)[16] with SbF_5, which were co-condensed through separate nozzles onto a surface cooled to liquid nitrogen temperature. Details of the method have been described

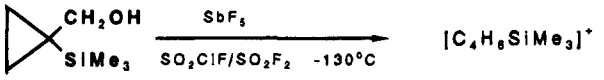

5 3

previously.[17] At −130 °C a yellow solution of (**3**) in SO_2ClF/SO_2F_2 was obtained. The ^{13}C-NMR spectrum (Figure 1, Table 1) measured at −128 °C shows three signals, one for the Si CH_3 groups at −5.2 ppm ($^1J_{CH}$ = 121 Hz, quartet), another for the quarternary carbon at 137.4 ppm, and a single signal at 48.9 ppm ($^1J_{CH}$ = 177 Hz, triplet) for the three methylene carbons. The ^{13}C- and ^1H-NMR data are summarized in Tables 1 and 2 together with the chemical shifts for cations **1** and **2** for comparison. Assignments of the NMR signals of **3** were made using ^1H-coupled and single-frequency ^1H-decoupled ^{13}C-NMR spectra, by comparison with the NMR spectral data of **1** and **2** and by means of chemical shift calculations (see below).

The chemical shifts of cation **3** show only a negligible variation with temperature. This is in contrast to the $[C_4H_7]^+$

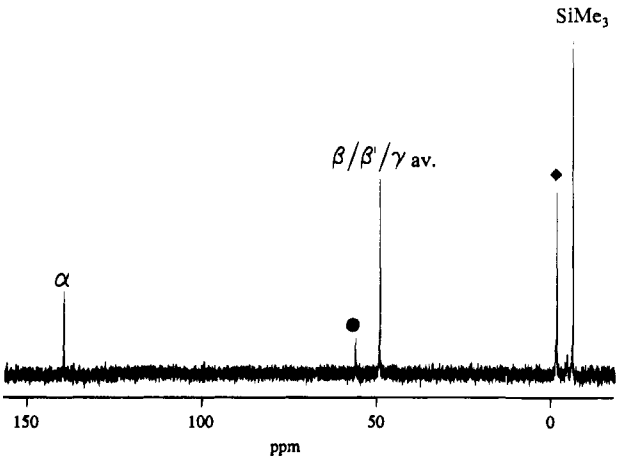

Figure 1. ^{13}C NMR (100.6 MHz) spectrum of cation **3** at −128 °C in SO_2ClF/SO_2F_2: (●) reference $\delta(NMe_4^+)$ = 55.65 ppm; (◆) $\delta(Me_3SiF)$ = −0.70 ppm.

Table 1. Experimental and Calculated ^{13}C-NMR Spectral Data for Cations **1**, **2**, **3**, and **4a**,**b**[a,b]

		C_α	$C_{\beta/\beta'}$	C_γ	$C_{\beta,\beta',\gamma}$ (av)	Me
1	expt[c]	108.2			57.6	
		(180)			(180)	
	GIAO-MP2//tzp/dz[d]	117.5	76.7	−15.4	46.0	
2	expt[e]	163.1	72.7	−2.8	48.7	25.4
					(177)	(130)
	GIAO-MP2//tzp/dz[d]	158.3	74.6	−5.3	48.0	29.2
3	expt[f]	137.4			48.9	−5.2
					(177)	
4a	GIAO-SCF//dzp/dz	140.3	68.8	−19.5	39.4	
	GIAO-SCF//tzp/dz	141.3	70.8	−20.2	40.5	
	GIAO-MP2//dzp/dz	128.5	75.6	−13.7	45.8	
	GIAO-MP2//tzp/dz	133.9	79.6	−14.5	48.2	
4b	GIAO-SCF//dzp/dz	71.1	72.9	249.2	131.7	
	GIAO-SCF//tzp/dz	74.5	73.3	253.4	133.3	
	GIAO-MP2//dzp/dz	86.3	84.4	224.9	131.2	
	GIAO-MP2//tzp/dz	92.1	87.0	235.2	136.4	

[a] Chemical shifts, δ, in ppm and measured coupling constants, $^1J_{CH}$, in Hz (in parentheses). [b] All calculations have been performed at MP2/6-31G*-optimized geometries. [c] Kelly, D. P.; Brown, H. C. *J. Am. Chem. Soc.* **1975**, *97*, 3897. [d] Reference 10. [e] Olah, G. A.; Prakash, G. K. S.; Donovan, D. J.; Yavari, J. *J. Am. Chem. Soc.* **1978**, *100*, 7085. Coupling constants: Olah, G. A.; Spear, R. J.; Hiberty, P. C.; Hehre, W. J. *J. Am. Chem. Soc.* **1976**, *98*, 7470. [f] 100.62 MHz, at −128 °C in SO_2ClF/SO_2F_2; internal reference $\delta(NMe_4^+)$ = 55.65 ppm (chemical shifts ± 0.02 ppm, coupling constants ± 1.6 Hz).

cation[18] for which a pronounced temperature dependence of the ^{13}C chemical shifts has been observed. This has been taken as *the* important piece of experimental evidence that besides the bicyclobutonium ion **1** small amounts of cyclopropylmethyl cation contribute to the dynamic averaging process. The temperature independence of the chemical shifts for cation **3** indicates that an analogous nondegenerate equilibrium is not very likely.

The ^1H-NMR spectrum of **3** (Table 2) measured at −128 °C shows a signal at 0.38 ppm with a relative intensity of 9 for the $Si(CH_3)_3$ protons. The geminal methylene protons give two singlet peaks, each with an intensity of 3 for the separately averaged signals for the *exo* (3.24 ppm)- and *endo* (4.05 ppm)-hydrogens at the methylene carbons. The specific *exo*/*endo* assignment is analogous to the assignment of the stereospecifically deuterium labeled bicyclobutonium cation $[C_4H_4D_3]^+$ investigated by Roberts et al.[19] and is confirmed by the

(16) Warner, P. M.; Le, D. *J. Org. Chem.* **1982**, *47*, 893.
(17) Lenoir, D.; Siehl, H.-U. In *Houben-Weyl Methoden der Organischen Chemie*; Hanack, M., Ed.; Thieme: Stuttgart, Germany, 1990; Vol. E19c, pp 26−32.
(18) Staral, J. S.; Yavari, I.; Roberts, J. D.; Prakash, G. K. S.; Donovan, D. J.; Olah, G. A. *J. Am. Chem. Soc.* **1978**, *100*, 8016.
(19) Brittain, W. J.; Squillacote, M. E.; Roberts, J. D. *J. Am. Chem. Soc.* **1984**, *106*, 7280.

Table 2. Experimental and Calculated ^{1}H-NMR Spectral Data for Cations **1**, **2**, **3**, and **4a**,**b**[a,b]

		$H_{\beta/\beta'}$ (*exo*)	H_γ (*exo*)	$H_{\beta/\beta'}$ (*endo*)	H_γ (*endo*)	av signals	other
1	expt[c]					4.21 (H_{exo}); 4.64 (H_{endo})	6.50 (H_α)
	GIAO-MP2//tzp/dz[d]	4.91	0.88	4.15	3.44	3.57 (H_{exo}); 3.91 (H_{endo})	6.19
2	expt[e]					3.89 ($H_{exo,endo}$)	2.87 (Me)
	GIAO-MP2//tzp/dz[d]	4.55	0.47	3.94	3.60	3.51 ($H_{exo,endo}$)	2.70
3	expt[f]					3.24 (H_{exo}); 4.05 (H_{endo})	0.38 (Me)
4a	GIAO-SCF//dzp/dz	4.62	0.21	3.92	3.04	3.15 (H_{exo}); 3.63 (H_{endo})	
	GIAO-SCF//tzp/dz	4.65	0.30	3.96	3.19	3.20 (H_{exo}); 3.70 (H_{endo})	
	GIAO-MP2//dzp/dz	4.59	0.48	3.96	3.28	3.22 (H_{exo}); 3.73 (H_{endo})	
	GIAO-MP2//tzp/dz	4.66	0.57	3.99	3.41	3.30 (H_{exo}); 3.80 (H_{endo})	
4b	GIAO-SCF//dzp/dz	4.76	10.28	4.57	9.69	6.60 (H_{exo}); 6.28 (H_{endo})	
	GIAO-SCF//tzp/dz	4.84	10.35	4.60	9.86	6.68 (H_{exo}); 6.35 (H_{endo})	
	GIAO-MP2//dzp/dz	5.07	9.28	4.85	8.67	6.47 (H_{exo}); 6.12 (H_{endo})	
	GIAO-MP2//tzp/dz	5.20	9.36	4.90	8.66	6.59 (H_{exo}); 6.15 (H_{endo})	

[a] Chemical shifts, δ, in ppm. [b] All calculations have been performed at MP2/6-31G*-optimized geometries. [c] Olah, G. A.; Jeuell, C. L.; Kelly, D. P.; Porter, R. D. *J. Am. Chem. Soc.* **1972**, *94*, 146. [d] Reference 10. [e] Olah, G. A.; Spear, R. J.; Hilberty, P. C.; Hehre, W. J. *J. Am. Chem. Soc.* **1976**, *98*, 7470. [f] 400.13 MHz, at −128 °C in SO_2ClF/SO_2F_2; internal reference $\delta(NMe_4^+) = 3.00$ ppm (chemical shifts ± 0.002 ppm).

calculated ^{1}H-NMR chemical shifts (see below). On specific ^{1}H decoupling at either CH_2 hydrogen resonance frequency, the triplet for the methylene carbon at 48.9 ppm collapses to a doublet.

In addition to the signals for cation **3**, the spectrum (Figure 1) shows additional peaks due to decomposition of the cation and formation of trimethylsilyl fluoride (Me_3SiF: $\delta(^{13}C) = -0.70$ ppm).[20] At −128 °C, the ^{1}H and ^{13}C signals of the cation loose about one-half the intensity within 30 min while the intensity of the Me_3SiF signal increases correspondingly.

The nonequivalence of the geminal methylene hydrogens excludes a planar cyclobutyl structure for cation **3**. Interconversion of the geminal hydrogens is not observed upon warming to −70 °C when rapid decomposition of the cation precludes further measurements. Similar to the parent $[C_4H_7]^+$ cation (**1**), the signals for the methylene protons of cation **3** show no geminal coupling.

A 3-fold symmetric structure for **3** would in principle account for the ^{1}H- and ^{13}C-NMR data. A 3-fold symmetric structure is however unlikely as theoretical considerations disfavor this high symmetry for the parent cation $[C_4H_7]^+$ [21] and also for $[C_4H_6SiH_3]^+$. A symmetric structure can be excluded with certainty by the observed equilibrium isotope effects (see below). The NMR data for **3** are consistent with a 3-fold degenerate set of less symmetric but rapidly equilibrating cation structures with the same effective time-averaged symmetry. Kinetic line broadening for the averaged CH_2 carbon signals of **3** was not observed at temperatures as low as −130 °C. This sets the upper limit for the barrier to methylene interconversion at about 4−5 kcal mol^{-1}.

In cation **3**, the three methylene carbons are averaged by a fast rearrangement process resulting in a single peak for the carbons, as it has been similarly observed for **1** and **2**. The shift for this averaged CH_2 signal is 48.91 ppm for **3**, 57.62 ppm for the mixture of the isomeric parent $[C_4H_7]^+$ cations,[22] and 48.69 ppm for the methylbicyclobutonium ion **2**.[23] The three CH_2 *endo* protons of **3** are averaged by the rearrangement process to give one peak at 4.05 ppm, and the three CH_2 *exo* protons average to one signal at 3.24 ppm. This compares with 4.21 and 4.64 ppm for the *exo*- and *endo*-hydrogen peaks in the parent $[C_4H_7]^+$ cation mixture.[24] For the methylbicyclobutonium ion (**2**), an additional conformational inversion of the cyclobutyl ring interchanges the *exo*- and *endo*-hydrogens and leads to a single averaged peak for all six methylene protons at 3.89 ppm.[25]

The transition state of the ring inversion is likely to correspond to a planar, α-substituted cyclobutyl cation (Scheme 1). A planar cyclobutyl cation with an α-hydrogen is too high in energy, so that ring inversion is not observed up to about −65 °C when fast decomposition occurs. With an α-methyl group in **2** the energy barrier for the cyclobutyl ring inversion is lowered due to better stabilization of the positive charge in the transition state by α-CH_3 compared to α-H. The interconversion of *exo*- and *endo*-methylene protons is fast on the NMR time scale, and only a single averaged peak for the six hydrogens is observed for **2**. This peak exhibits kinetic line broadening at lower temperatures.[26] The two dynamic processes, the ring interconversion leading to interconversion of the *exo*- and *endo*-hydrogens and the methylene rearrangement averaging the β- and γ-positions, cannot be separated, and only two broad and unstructured peaks were observed at −150 °C.[27]

The fact that two separate ^{1}H-NMR signals for the *exo*- and *endo*-methylene protons are observed for cation **3** shows that the energy barrier for conformational ring inversion is higher than the corresponding barrier for the methylbicyclobutonium ion (**2**). This is in accord with earlier findings that the α-trimethylsilyl group stabilizes a positive charge less than an α-methyl group. It confirms that **3** is intermediate in between the parent bicyclobutonium ion (**1**) and the methylbicyclobutonium ion (**2**) in terms of structure, dynamics, and charge delocalization.

Equilibrium Isotope Effects

Equilibrium isotope effects have been established as a sensitive probe for the nature of carbocations in superacid solutions.[28] To obtain more detailed information on the dynamic process in cation **3** we have investigated equilibrium isotope effects in the NMR spectra of deuterated cations **3**-d_1 and **3**-d_2. A mixture of stereoisomeric CHD-monodeuterated $[C_4H_5DSiMe_3]^+$ cations, *exo*-**3**-d_1 and *endo*-**3**-d_1, was obtained by

(20) Harris, R. K.; Kimber, B. J. *J. Magn. Reson.* **1975**, *17*, 174.
(21) (a) Trindle, C.; Sinanoglu, O. *J. Am. Chem. Soc.* **1969**, *91*, 4054. (b) Saunders, M.; Laidig, K. E.; Wiberg, K. B.; Schleyer, P. v. R. *J. Am. Chem. Soc.* **1988**, *110*, 7652.
(22) Kelly, D. P.; Brown, H. C. *J. Am. Chem. Soc.* **1975**, *97*, 3897.
(23) Olah, G. A.; Prakash, G. K. S.; Donovan, D. J.; Yavari, J. *J. Am. Chem. Soc.* **1978**, *100*, 7085.
(24) Olah, G. A.; Jeuell, C. L.; Kelly, D. P.; Porter, A. D. *J. Am. Chem. Soc.* **1972**, *94*, 146.
(25) Olah, G. A.; Spear, R. J.; Hiberty, P. C.; Hehre, W. J. *J. Am. Chem. Soc.* **1976**, *98*, 7470.
(26) Kirchen, R. P.; Sørensen, T. S. *J. Am. Chem. Soc.* **1977**, *99*, 6687.
(27) Gottaut, I.; Siehl, H.-U. Unpublished results. Gottaut, I. Diplomarbeit, University of Tübingen, 1990.
(28) For a review, see: Siehl, H.-U. *Adv. Phys. Org. Chem.* **1987**, *23*, 63−163.

Scheme 1. Two Equilibration Possibilities for Bicyclobutonium Ions $[C_4H_6R]^+$ [a]

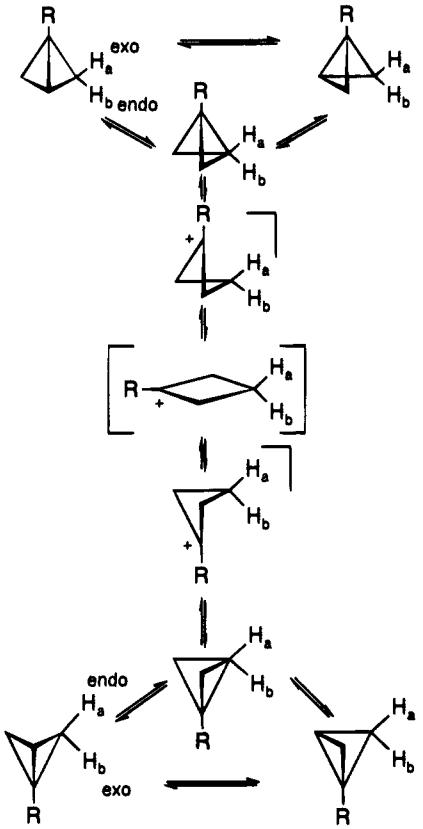

[a] The three CH_2 carbons are averaged by a 3-fold degenerate methylene rearrangement. Three protons H_a are averaged with three protons H_b by a conformational equilibrium process via planar cyclobutyl cation structures. For R = H and $SiMe_3$, the conformational inversion is not observed. (The + symbol for the positive charge is omitted for the bicyclobutonium ions).

reaction of α-CHD-monodeuterated (1′-(trimethylsilyl)cyclopropyl)methanol with SbF_5. The CD_2-dideuterated cation $[C_4H_4D_2SiMe_3]^+$ (**3**-d_2) was generated from α-CD_2-(1′-(trimethylsilyl)cyclopropyl)methanol. The ^{13}C- and ^1H-NMR spectra of solutions of **3**-d_1 as well as mixtures of **3**-d_1/**3**-d_0 and **3**-d_2/**3**-d_0 cations were investigated at various temperatures.

Deuteration does not affect the chemical shift of the Si methyl groups. For the quarternary carbon C_α of the *exo*-/*endo*-**3**-d_1 cations, two signals, 0.055 ppm upfield and 0.1676 ppm downfield from the corresponding signal of **3**-d_0, are observed at −128 °C. We attribute these shifts to intrinsic deuterium-induced shifts on the chemical shift of the α-carbon which are different for the *exo*- and *endo*-CHD cations. In the CD_2-dideuterated cation **3**-d_2 the intrinsic shift for the quarternary carbon is about the arithmetic mean of the d_1-induced shifts, 0.075 ppm downfield relative to **3**-d_0 at −125 °C.

The NMR signals for the averaged methylene positions in the deuterated cations either split into pairs or show large shifts relative to the d_0 cation. The splitting of the methylene signal in the d_1 and d_2 cations into CHD/CH_2 and CD_2/CH_2 peak pairs occurs because the degeneracy of the equilibrium is lifted by the isotopic substitution and the shifts for deuterated and non-deuterated methylene groups do no longer average at the same position. In the ^1H-NMR spectrum of **3**-d_2 only the CH_2 part of the CD_2/CH_2 peak pair can be detected. Due to low sensitivity because of line broadening caused by unresolved deuterium couplings and relaxation effects, the CHD and CD_2 peaks could not be observed in the ^{13}C-NMR spectrum. Most valuable for the determination of the relative size and the relative

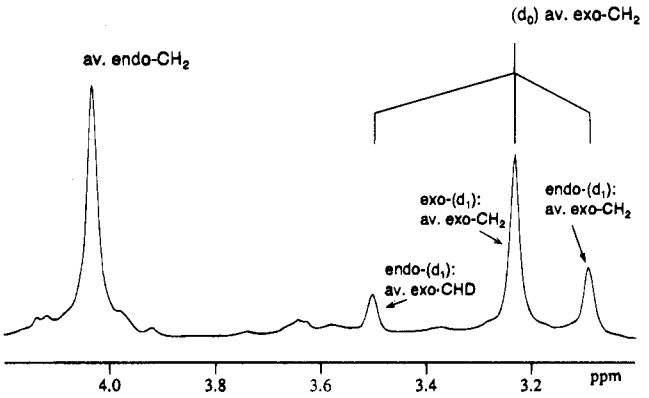

Figure 2. ^1H NMR (400.13 MHz) spectrum of a mixture of cation **3** and CHD-labeled **3**-d_1 at −128 °C in SO_2ClF/SO_2F_2: reference $\delta(NMe_4^+)$ = 3.00 ppm; signal of $SiMe_3$ (0.38 ppm) is not shown.

sign of the equilibrium isotope effects are the ^{13}C-NMR and the ^1H-NMR spectra of monodeuterated cation **3**-d_1. The displacements of the CH_2 signals of **3**-d_2 relative to those of **3**-d_0 in the ^1H- and ^{13}C-NMR spectra supply further information. The shifts of the peaks of the deuterated cations **3**-d_1 and **3**-d_2 relative to those of **3**-d_0 decrease with increasing temperature. This is characteristic for equilibrium isotope effects on NMR spectra of degenerate fast rearranging systems. The occurrence of equilibrium isotope effects excludes a 3-fold symmetric structure and proves that in solution cation **3** is best described as a set of degenerate structures undergoing a dynamic rearrangement which is fast on the NMR time scale at all temperatures investigated. Conformational inversion does not occur under the conditions of the experiment, since separate signals are observed for the *exo*- and *endo*-monodeuterated cations **3**-d_1. At −128 °C the averaged CH_2 carbon signals of the two isomeric d_1 cations are separated by 3.27 ppm. The isotope effects of the *exo*- and *endo*-deuterated isomers have different signs, and the observed relative shifts with respect to the nondeuterated cation **3**-d_0 are different in magnitude, reminiscent to the effects observed[4] and calculated[29] for the parent cation (**1**). The specific assignment of the CH_2 carbon peaks to the *exo*- and *endo*-d_1 cations is based on the *exo*/*endo* assignment of the methylene signals in the ^1H-NMR spectra of **3** and **3**-d_1 (Figure 2).

In a mixture of *exo*-/*endo*-**3**-d_1 and **3**-d_0 at −128 °C, the averaged CH_2 carbon signal of the *endo*-d_1 cation is shifted 3.1 ppm upfield relative to the averaged CH_2 peak of the nonlabeled cation **3**-d_0 while the averaged CH_2 carbon signal of the *exo*-**3**-d_1 cation is shifted downfield relative to that of **3**-d_0 by only 0.17 ppm. In the ^1H-NMR spectra of the d_1 cation measured at −128 °C (Figure 2) only the peak for the averaged *exo*-methylene protons shows a sizable equilibrium isotope effect while any isotopic splitting for the *endo*-proton peak is too small to be observed. The signal for the *exo*-methylene hydrogens in the *endo*-deuterated cation (*endo*-**3**-d_1) splits into two peaks. The relative intensity is 1:2 for the downfield and the upfield peak, and the ratio of the isotopic shifts relative to **3**-d_0 is 2:1 for the downfield and the upfield peaks. The peak for the *exo*-CHD hydrogen with relative intensity of 1 is shifted about 0.26 ppm downfield, the other peak for the *exo*-CH_2 hydrogens with intensity of 2 is shifted about 0.14 ppm upfield relative to the peak of the nonlabeled cation. Taking into account a correction of about 0.02 ppm as an intrinsic upfield shift for the *exo*-CHD hydrogen caused by the geminal *endo*-deuterium, the equilibrium

(29) Saunders, M.; Laidig, K. E.; Wolfsberg, M. *J. Am. Chem. Soc.* **1989**, *111*, 8989.

isotope splitting for the signal pair of the averaged *exo*-CHD/*exo*-CH_2 hydrogens in *endo*-**3**-d_1 is 0.42 ppm.

A correlation of the observed ^{1}H-NMR methylene signals for *exo*-/*endo*-**3**-d_1 with the calculated shifts of a model cation **3a** is shown in Scheme 2. The splitting pattern observed for the *exo*-methylene signals is readily interpreted in terms of isotope effect theory. Two hydrogens and one deuterium are equilibrated between two bonding sites, the doubly populated β-position and the singly populated γ-position which have different C−H bond force constants and thus different contributions to the zero point vibrational energy. The heavier isotope deuterium prefers the position with the larger bond force constant.[30] The intensity ratio of the splitting pattern for the *exo*-methylene signal of *endo*-**3**-d_1 shows that *endo*-deuterium is preferred at the lowfield site, which according to GIAO-MP2 calculations for model cation **4a** (Table 2) is the site of the *endo*-β-hydrogens in a static bicyclobutonium structure (**4a,** δH_β: 3.99 ppm (tzp/dz)). The hydrogens are preferred at the highfield site which according to the calculations is the *endo* H-position at the hypercoordinated C_γ carbon(**4a**, $\delta H\gamma$: 3.19 ppm (tzp/dz)). The force constant for the *endo*-C−H bond at the hypercoordinated C_γ carbon is therefore lower than the *endo*-C−H bond force constant at the tetracoordinated β-methylene carbons. This is confirmed by quantum chemical calculations (see below).

In the ^{1}H-NMR spectra of *exo*-/*endo*-**3**-d_1 another peak with relative intensity of 2 can be assigned to the *exo*-CH_2 hydrogens in *exo*-**3**-d_1. This peak has virtually the same shift as the unperturbed *exo*-CH_2 hydrogens in **3**-d_0 and contributes to the intensity of the *exo*-**3**-d_0 peak in the spectrum of the mixture of **3**-d_1/**3**-d_0 cations shown in Figure 2. Taking into account the large calculated shift difference for the *exo*-β-/γ-hydrogens (4.66 − 0.57 = 4.09 ppm) in the model cation **4a** compared to the difference calculated for the *endo*-β-/γ-hydrogens (3.99 − 3.41 = 0.58 ppm) (GIAO-MP2//tzp/dz), it follows that any isotope effect caused by *exo*-deuterium is small in contrast to the large effect caused by deuterium in the *endo* position. This interpretation is in full accord with the ^{13}C-NMR spectrum of the mixture of *exo*-/*endo*-**3**-d_1 cations, which clearly shows the different magnitude of the isotope effects for *exo*- and *endo*-deuterium and in addition their different signs.

In the ^{13}C-NMR spectrum of a mixture of CD_2-**3**-d_2 and **3**-d_0 cation the CH_2 groups of the d_2 cation shows at −128 °C an upfield shift of 2.82 ppm relative to that of the d_0 cation. This is about the sum of the opposite effects in the *exo*-/*endo*-monodeuterated cations. The CD_2 multiplet which should be downfield of the d_0 signal is not visible due to low sensitivity. In the ^{1}H-NMR spectra of a mixture of d_2 and d_0 cations only the upfield peak for the *exo*-methylene hydrogens shows a sizable isotope effect. At −128 °C the averaged CH_2 signal of the d_2 cation is shifted upfield by 0.13 ppm relative to the **3**-d_0 signal.

The different isotope effects observed for *exo*- and *endo*-deuterium reveal that the relative differences for the force constants between the doubly populated β-methylene and the singly populated C_γ site are opposite for the *exo*- and *endo*-C−H bonds. While the vibrational force constants for the *endo*-C−H bonds are higher at the β-methylene position than at the γ-position, the *exo*-C−H bond at the γ-carbon is somewhat stiffer compared to the *exo*-C−H bonds at the β-methylene carbons.

(30) For general treatments of isotope effects, see: (a) Melander, L.; Saunders, W. H., Jr.; *Reaction Rates of Isotopic Molecules*; Wiley: New York, 1980. (b) Collins, C. J.; Bowman, N. S., Eds.; *Isotope Effects in Chemical Reactions*; ACS Monograph No. 167; Van Nostrand Reinhold: New York, 1970. (c) Wolfsberg, M. *Acc. Chem. Res.* **1972**, *7*, 225. (d) Willi, A. V. *Isotopeneffekte bei chemischen Reaktionen*; Georg Thieme Verlag: Stuttgart, Germany, 1983.

Scheme 2. Schematic ^{1}H NMR Spectra of the Methylene Region (a) Calculated for Static **4a**, (b) Averaged for **4a**, and (c) Observed for a Mixture of *exo*- and *endo*-**3**-d_1 (Expanded Scale)

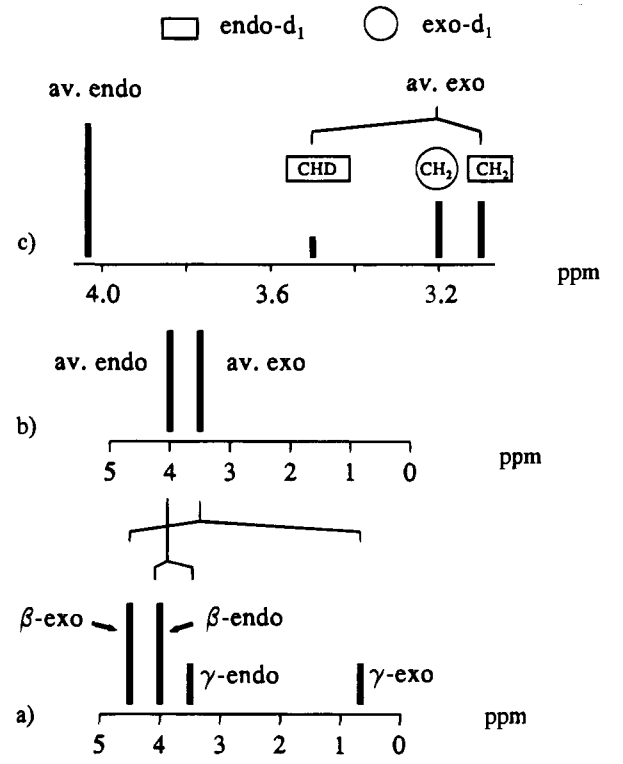

This is direct experimental evidence that cation **3** has the bridged bicyclobutonium structure **3a** and that other structures can be excluded. The isotope effects for **3** are clearly distinct from those expected for a degenerate set of cyclopropylmethyl structures **3b** according to experimental observations for other substituted cyclopropylmethyl cations.[31,32] The isotope effects for **3** are also different from those observed for triply degenerate sets of puckered 1-substituted cyclobutyl cations.[9,32] For a degenerate set of structures **3b**, the same isotope effects for *endo*- and *exo*-deuterium should be observed according to calculations for the parent cyclopropylmethyl cation.[29] For the pentacoordinated γ-carbon in **3a,** it is conceivable and has been verified for the parent bicyclobutonium ion theoretically[29] that *exo* and *endo*-C−H bonds have different force constants. The C_α−C_γ bridging interaction lowers the electron density in the *endo* C_γ−H bond, due to a back lobe interaction (cross ring hyperconjugation) with the formally positive charged carbon C_α. This results in a lower force constant for the *endo*-C−H bond at the bridging carbon compared to the other *endo*-C−H bonds at the tetracoordinated carbons. According to the experimental results the *exo*-C−H bond at the pentacoordinated carbon of **3** has a slightly larger force constant compared to *exo*-C−H bonds at the tetracoordinated carbons. This may be due either to hindrance of bending vibrations caused by cross ring sterical interaction with the bulky trimethylsilyl substituent at C_α or to the unique apical position of the *exo*-H at the pentacoordinated carbon.

Quantum Chemical Calculations

To further support the interpretation of the NMR spectroscopic results we have performed quantum chemical ab initio

(31) Siehl., H.-U.; Koch, E.-W. *J. Chem. Soc., Chem. Commun.* **1985**, 496.

(32) Schneider, J. Ph.D. Thesis, University of Tübingen, 1989.

Table 3. Calculated Absolute Energies and Relative Energies (Including Zero Point Vibrational Energy (ZPE)) for Cations **4a,b**[a]

	E		*ΔE*			
	SCF/6-31G* (ZPE) [NIMAG]	MP2/6-31G* (ZPE) [NIMAG][b]	SCF/6-31G*	SCF/6-31G* + ZPE	MP2/6-31G*	MP2/6-31G* + ZPE
4a	−445.30550 (0.12159) [0]	−445.89004 (0.11606) [0]	−0.3	0	−3.4	−2.8
4b	−445.30500 (0.12041) [0]	−445.88455 (0.11499) [1]	0	−0.4	0	0

[a] Absolute energies in hartrees; relative energies in kcal mol^{-1}. Calculations have been performed at geometries optimized at the same level of theory. The inner shell electrons have been excluded from the calculation of the MP2 correlation energy. [b] Number of imaginary frequencies obtained in the frequency calculations.

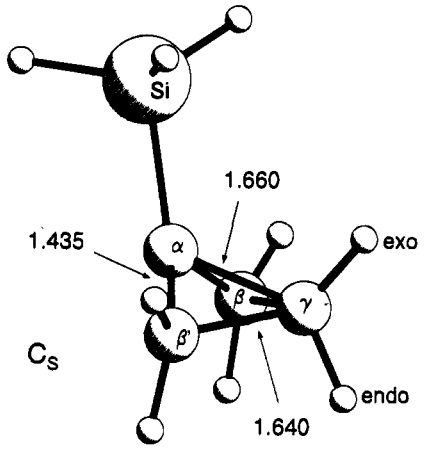

Figure 3. Calculated MP2/6-31G* geometry of cation **4a** with selected bond lengths in Å.

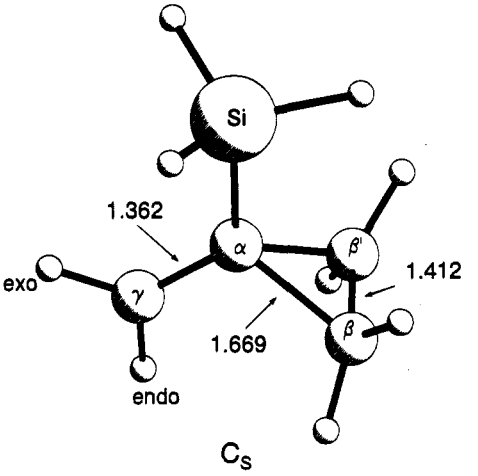

Figure 4. Calculated MP2/6-31G* geometry of cation **4b** with selected bond lengths in Å.

calculations for the structure and NMR chemical shifts of the silyl-substituted bicyclobutonium and cyclopropylmethyl cations. For computational reasons, model compounds **4a,b** obtained by replacing in **3a,b** the methyl groups by hydrogens have been studied instead of the experimentally investigated system $[C_4H_6Si(CH_3)_3]^+$. The geometries for **4a,b** were optimized at the HF/6-31G* and MP2/6-31G* levels of theory.[33] Table 3 reports the calculated energies; Figures 3 and 4 show the MP2/6-31G* optimized structures.

Unlike for the parent system, frequency calculations at the HF/6-31G* level reveal that both the bicyclobutonium cation **4a** and the cyclopropylmethyl cation **4b** correspond to minima on the potential energy surface. At the same level of theory, the cyclopropylmethyl structure **4b** is predicted to be marginally (−0.4 kcal mol^{-1}, HF/6-31G* including zero point energy (ZPE) corrections) more stable than **4a**. At the correlated level (MP2/6-31G* including ZPE), the energetic order is reversed and the bicylobutonium structure **4a** is calculated to be 2.8 kcal mol^{-1} more stable than the cyclopropylmethyl structure **4b**. Furthermore, frequency calculations show that at the MP2 level only structure **4a** represents a local minimum, while one, although small, imaginary frequency, is obtained for **4b**. Hence, the (1′-silylcyclopropyl)methyl cation is predicted to be a transition state, probably for the interconversion of two degenerate bicyclobutonium structures. However, the small magnitude of the imaginary frequency (57i cm^{-1}) as well as the low energetic separation between **4a** and **4b** indicates that the potential energy surface is very flat, as it has been also found for the parent and the methyl-substituted system, $C_4H_7^+$ and $C_4H_6CH_3^+$, respectively.[10]

Table 4. Selected Calculated Bond Lengths (in Å) of Cations **1**, **4a**, and **2** As Obtained at the MP2/6-31G* Level[a]

	$C_\alpha-C_\gamma$ (bridge)	$C_\alpha-C_\beta$	$C_\beta-C_\gamma$	$C_\gamma-H_{endo}$	$C_\gamma-H_{exo}$
				$C_\beta-H_{endo}$	$C_\beta-H_{exo}$
1	1.654	1.426	1.650	1.087	1.084
				1.086	1.086
4a	1.661	1.435	1.641	1.088	1.085
				1.088	1.086
2	1.708	1.436	1.630	1.088	1.085
				1.087	1.086

[a] Data for **1**; see refs 10 and 36. For **2**, see ref 10.

The main geometrical features calculated for structure **4a** closely resemble those of the parent system (**1**)[4] and the methyl-substituted ion (**2**)[10] (see Table 4). The $C_\alpha-C_\gamma$ bridging distance in the 1-substituted cations $[C_4H_6R]^+$ increases from 1.654 Å in **1** (R = H) to 1.661 Å in **4a** (R = SiH_3) and 1.708 Å in **2** (R = CH_3), indicating a decreasing demand for cross ring hypercoordinative charge stabilization consistent with the better capability of SiH_3 and in particular CH_3 to stabilize a positive charge in α-position.

The $C_\alpha-C_\beta$ bonds adjacent to the cationic center for all three cations are short (1.426 Å for **1**, 1.435 Å for **4a**, and 1.436 Å for **2**), while the $C_\beta-C_\gamma$ distances are calculated to be 1.650 Å for **1**, 1.641 Å for **4a**, and 1.630 Å for **2**, respectively. The results for these geometrical parameters can be rationalized by contributions of hyperconjugative homoallyl type no bond resonance structures, consistent with the finding that shorter $C_\alpha-C_\beta$ distances correlate with longer $C_\beta-C_\gamma$ bonds.

(33) For a description of the HF-SCF and the MP2 method as well as the 6-31G* basis set, see for example: Hehre, W.; Radom, L.; Schleyer, P. v. R.; Pople, J. A. *Ab initio Molecular Orbital Theory*; Wiley: New York, 1986. All calculations of geometries and frequencies have been performed with the Gaussian 90 and Gaussian 92 program packages (Frisch, M. J.; Trucks, G. W.; Head-Gordon, M.; Gill, P. M. W.; Wong, M. W.; Foresman, J. B.; Johnson, B. G.; Schlegel, H. B.; Robb, M. A.; Replogle, E. S.; Gomperts, R.; Andres, J. L.; Raghavachari, K.; Binkley, J. S.; Gonzalez, C.; Martin, R. L.; Fox, D. J.; Defrees, D. J.; Baker, J.; Stewart, J. J. P.; Pople, J. A. *Gaussian 92*, Revision; Gaussian, Inc.: Pittsburgh, PA, 1992).

Table 5. Calculated Natural Charges for Hydrogens and Carbon Fragments of Cations **1**, **4a**, and **2**

	R	H_γ *endo* H_β *endo*	H_γ *exo* H_β *exo*	C_α–R	$(CH_2)_3$	γ-CH_2	β-CH_2
1	H	0.353	0.304	0.322	0.678	0.219	0.229
		0.287	0.294				
4a	SiH_3	0.355	0.296	0.367	0.633	0.209	0.212
		0.281	0.283				
2	Me	0.344	0.293	0.404	0.596	0.209	0.193
		0.288	0.285				

Table 6. Calculated Wiberg Bond Indixes for Cations **1**, **4a**, and **2**

	C_γ–H_{endo} C_β–H_{endo}	C_γ–H_{exo} C_β–H_{exo}	C_α–C_γ (bridge)	C_α–C_β	C_β–C_γ
1	0.83	0.89	0.48	1.18	0.78
	0.90	0.90			
4a	0.82	0.89	0.47	1.17	0.79
	0.90	0.90			
2	0.84	0.90	0.40	1.15	0.82
	0.89	0.90			

The methylene C–H bonds show only minor variation with the substituents. The *endo* bonds found for all cations are somewhat longer than the geminal *exo*-C–H bonds. The difference is most pronounced for the C–H bonds at the pentacoordinated carbon (C_γ–H_{endo} = 1.088 Å and C_γ–H_{exo} = 1.084 Å for **4a**). The *endo*-C–H bonds at the pentacoordinated carbon C_γ are marginally longer than the other *endo*-C–H bonds while the *exo*-C–H bonds at C_γ are calculated to be shorter than the *exo*-C–H bonds at the β-carbons. This data qualitatively agree with the results from the isotope effect experiments.

The calculated natural charges from an NBO analysis[34] (Table 5) and the Wiberg bond indixes[35] (Table 6) illustrate the analysis of the geometry data and also support the interpretation of the isotope effects. It is known for carbocations in general and has been specifically demonstrated for bicyclobutonium ions that the positive charge is found largely on the hydrogens.[36] The *endo*-C_γ–H bond at the pentacoordinated carbon is more involved in the stabilization of the positive charge by bridging than the *exo*-C_γ–H bond. Significantly more charge is located at the *endo*-hydrogens at C_γ (*endo*-H_γ 0.353, 0.355, and 0.344 in **1**, **4a**, and **2**) compared to the other methylene hydrogens (0.280–0.304). The *endo*-C_γ–H bond in **1**, **4a**, and **2** has a lower bond index (0.82–0.84) than all other methylene C-H bonds (0.89–0.90).

More than one-half of the positive charge is localized at the CH_2 groups of the cyclobutyl ring (0.678, 0.633, and 0.596 in **1**, **4a**, and **2**). The charge delocalization into the ring decreases with increasing donor strength of the substituent at C_α. The charges calculated for the β- and γ-methylene groups are similar, indicating about equal delocalization of positive charge into these positions. The bond indexes of the C_α–C_γ bridging bond decrease from 0.48 to 0.47 and 0.40 in **1**, **4a**, and **2** in accord with the decreasing demand for cross ring charge stabilization. The concomitant bond index decrease for the C_α–C_β bond (1.18, 1.17, and 1.15) and the increase for the C_β–C_γ bond (0.78, 0.79, and 0.82) parallel the change of the geometrical parameters in the same order **1**, **4a**, and **2**. Similar to those for **1** and **2**, the hybridization factor sp^x for **4a** is 3.1 for the β- and γ-carbons while 2.8 is calculated for the formal cationic center carbon C_α. The deviation from the standard sp^2 hybridization for trivalent carbocations is the result of the unusual geometry of bicyclobutonium ions.

To confirm the interpretation of the NMR spectra for **3** and to link the calculated results for the structure with experimental data, we have computed the NMR chemical shifts for cations **4a**,**b** using the gauge-including atomic orbital (GIAO)-SCF[37] and GIAO-MP2[38] methods. All calculations[39] have been performed for MP2/6-31G*-optimized structures using double- and triple-ζ polarization (dzp and tzp, respectively) basis sets from ref 40. For computational reasons, a double-ζ (dz) basis set has been used in all calculations for the hydrogens. Tables 1 and 2 summarize the GIAO-SCF- and GIAO-MP2-calculated ^{13}C- and ^1H chemical shifts for **4a**,**b** together with corresponding results from ref 10 for the parent systems and the methyl substituted cations.

The calculated ^{13}C chemical shifts for the 1-silylbicyclobutonium cation structure **4a** are in excellent agreement with the experimental shifts observed for **3**, while this is not the case for the computed shifts of the 1′-silylcyclopropylmethyl cation structure **4b**. The averaged shift of the methylene carbons of **4a** is calculated at the GIAO-MP2 level to be 48.2 ppm, which has to be compared to the experimental value of 48.9 ppm for **3**. For the quaternary carbon, the calculated value is 133.9 and the experimental value is 137.4 ppm. These small differences (average for C_β, $C_{\beta'}$, and C_γ, 0.7 ppm; C_α, 3.5 ppm) between the calculated chemical shifts for the $[C_4H_6SiH_3]^+$ model bicyclobutonium structure **4a** and the experimentally observed chemical shifts for the $[C_4H_6SiMe_3]^+$ structure **3** strongly support the interpretation that cation **3** has the 1-(trimethylsilyl)-bicyclobutonium ion structure **3a** analogous to **4a**. Consistent with the finding that **4b** does not represent a local minimum on the potential energy surface, this good agreement between theoretical and experimental shifts confirms that the 1′-(trimethylsilyl)cyclopropylmethyl ion structure does not contribute to the observed chemical shifts.

These conclusions are also supported by a comparison of calculated and experimental ^1H chemical shifts. Again, there is only a good agreement between the computed values for **4a** and those measured for **3**. The differences between the observed and calculated shifts are 0.06 and 0.25 ppm for the averaged *exo*- and *endo*-hydrogen signals, respectively.

Rather large different shifts are calculated for the *exo*-hydrogens at the tetracoordinated β-carbon (4.66 ppm, MP2//tzp/dz) and the pentacoordinated γ-carbon (0.57 ppm, MP2//tzp/dz). The difference amounts to 4.1 ppm, while for the corresponding *endo*-hydrogens, only a shift difference of 0.58 ppm is obtained in the calculations (3.99 ppm for the *endo*-H at C_β and 3.41 ppm for the *endo*-H at the γ-carbon). The unusually low value of 0.57 ppm for the *exo*-hydrogen at the γ-carbon might be explained by the atypical position of this proton at the pentacoordinated carbon.

(34) (a) Reed, A. E.; Weinstock, R. B.; Weinhold, F. *J. Chem. Phys.* **1985**, *83*, 735. (b) Reed, A. E.; Curtis, L. A.; Weinhold, F. *Chem. Rev.* **1988**, *88*, 899.

(35) Wiberg, K. B. *Tetrahedron* **1968**, *24*, 1083.

(36) Wiberg, K. B.; Shobe, D.; Nelson, G. L. *J. Am. Chem. Soc.* **1993**, *115*, 10645. Note that an inverse labeling for the *exo*- and *endo*-hydrogens is used in this reference.

(37) London, F. J. *Phys. Radium* **1937**, *8*, 397. Hameka, H. *Mol. Phys.* **1958**, *1*, 203. Ditchfield, R. *Mol. Phys.* **1974**, *27*, 789. Wolinski, K.; Hinton, J. F.; Pulay, P. *J. Am. Chem. Soc.* **1990**, *112*, 8251. Häser, M.; Ahlrichs, R.; Baron, H. P.; Weis, P.; Horn, H. *Theor. Chim. Acta* **1992**, *83*, 455.

(38) Gauss, J. *Chem. Phys. Lett.* **1992**, *191*, 614. Gauss, J. *J. Chem. Phys.* **1993**, *99*, 3629.

(39) All GIAO-SCF and GIAO-MP2 calculations have been performed with the quantum chemical program package ACES II (Stanton, J. F.; Gauss, J.; Watts, J. D.; Lauderdale, W. J.; Bartlett, R. J. *ACES II*; University of Florida: Gainesville, FL, 1993). For a detailed description of ACES II, see: Stanton, J. F.; Gauss, J.; Watts, J. D.; Lauderdale, W. J.; Bartlett, R. J. *Int. J. Quantum Chem. Symp.* **1992**, *26*, 879.

(40) Schäfer, A.; Horn, H.; Ahlrichs, R. *J. Chem. Phys.* **1992**, *97*, 2571. Note that due to program restrictions the full set of Cartesian *d*-functions has been used in all chemical shift calculations.

The effects of electron correlation and basis set on the calculated ^{13}C and ^{1}H chemical shifts are noticeable for both model structures **4a** and **4b**, although for the latter, no experimental data are available for comparison. The shifts of the carbons with the formal positive charge, i.e. C_α in **4a** and C_γ in **4b**, are described as too deshielded at the GIAO-SCF level, while for the other carbons, the opposite is found. Comparison of the shifts for **4a** with the experimental results for **3** indicates that the GIAO-SCF//tzp/dz value for C_α is about 4 ppm too deshielded, while the averaged shielding for the methylene group is underestimated by about 8−10 ppm at the SCF level. For both shieldings, an improvement is obtained at the correlated level with remaining errors of about 3.5 ppm for C_α and less than 1 ppm for the averaged value of C_β and C_γ. As seen in earlier studies,[41] these results demonstrate again the importance of electron correlation in accurate calculations of NMR chemical shifts for carbocations with extended delocalization of the positive charge.

These results for **3** and **4** should be compared to those for the parent $[C_4H_7]^+$ system where a discrepancy between experimental and calculated shifts has been found (experimental: C_α 108.2 ppm; average of C_β, $C_{\beta'}$, and C_γ, 57.6 ppm; GIAO-MP2//tzp/dz: C_α 117.5 ppm; average of C_β, $C_{\beta'}$, and C_γ, 46.0 ppm; see ref 10) and taken as strong evidence that besides a set of rapidly equilibrating bicyclobutonium structures as major component (75−85%) also a degenerate set of cyclopropylmethyl cation structures contributes to the averaging process.

For the $[C_4H_6CH_3]^+$ cation system a similar equilibration process has been postulated between the main 1-methylbicyclobutonium cation (**2a**) and a so far unknown minor species.[11] However, most experimental studies[7,8,9] as well as quantum chemical calculations[10] do no lend support to this idea. The differences between the experimental (C_α, 163.1 ppm; average for C_β, $C_{\beta'}$, and C_γ, 48.7 ppm; CH_3, 25.4 ppm) and the calculated GIAO-MP2//tzp/dz (C_α, 158.3 ppm; average for C_β, $C_{\beta'}$, and C_γ, 48.0 ppm; CH_3, 29.2 ppm) shift data are 0.7 ppm for the methylene carbons and 4.8 ppm for the quarternary carbon, respectively. These deviations are so small that it is completely sufficient to consider only interconverting degenerate bicyclobutonium ion structures **2a** to account for the experimental NMR spectra of $C_4H_6CH_3^+$ cations.

Conclusions

A trimethylsilyl-substituted hypercoordinated carbocation $C_4H_6SiMe_3^+$ has been generated by reaction of (1′-(trimethylsilyl)cyclopropyl)methanol with SbF_5 at low temperature. The experimental ^{13}C- and ^{1}H-NMR data as well as the equilibrium isotope effects observed for the CHD-monodeuterated and the CD_2-dideuterated cations are consistent with a degenerate, interconverting set of bicyclobutonium cation structures. No evidence for contributions of the corresponding cyclopropylmethyl cation structure to this dynamical process could be found. Unlike for the methyl-substituted cation $C_4H_6CH_3^+$, ring inversion is not observed and separate signals for the *endo*- and *exo*-hydrogens are detected. The interpretation of the experimental results is strongly supported by quantum chemical ab initio calculations of structure and NMR chemical shifts. MP2/6-31G* geometry optimizations predict only the bicyclobutonium cation structure **4a** to be a minimum on the potential energy surface, while the cyclopropylmethyl cation structure **4b** corresponds to a transition state for the interconversion of two degenerate bicyclobutonium structures. The chemical shifts for the bicyclobutonium cation **4a** as calculated at the GIAO-MP2//tzp/dz level are in good agreement with the experimental results. This agreement gives further support to the conclusion that no second (minor) species has to be invoked to explain the experimental facts.

The structure and dynamics and charge delocalization of 1-substituted cyclobutyl cations are strongly influenced by the electronic properties of the substituent at the α-carbon. The properties of the 1-silyl-substituted bicyclobutonium ion **3** are in between those of the parent and the 1-methyl substituted bicyclobutonium ion. Similar to the $C_4H_6CH_3^+$ cation **2**, no other isomer contributes to the observed NMR spectra of **3**. In contrast to the methyl-substituted cation but similar to the parent bicyclobutoniumion **1**, cation **3** undergoes no conformational ring inversion; hence, different chemical shifts and different equilibrium isotope effects are observed for the *exo*- and *endo*-hydrogens.

Experimental Section

(1′-(Trimethylsilyl)cyclopropyl)carboxylic Acid (7). The synthesis was done as described.[42] ^{13}C-NMR (62.90 MHz, $CDCl_3$, 27 °C): δ −2.62 (q, $^{1}J_{CH}$ = 119 Hz, CH_3), 10.60 (s, quarternary carbon of cyclopropane ring), 13.28 (t, $^{1}J_{CH}$ = 165 Hz, CH_2 cyclopropane ring), 183.4 (s, carbonyl carbon). ^{1}H-NMR: δ −0.04 (CH_3), 0.8/1.2 (ring methylene protons). FT-IR (KBr, solid): 843 (s, ν_{def} cyclopropane ring), 1248 (s, ν_{def} $Si(CH_3)_3$ group), 1676 (s, ν_{sym} carbonyl group), 2500−3400 (m, ν_{sym} O−H bond).

(1′-(Trimethylsilyl)cyclopropyl)methanol (5). A solution of 4.18 g (0.026 mol) of (1′-(trimethylsilyl)cyclopropyl)carboxylic acid (**7**) in 20 mL of dry ether was added to a stirred suspension of 1.1 g (0.02 mol) of lithium aluminium hydride in 40 mL of dry ether, and the mixture was stirred for 3 h. The solution was cooled with ice and 1.1 mL of water, 1.1 mL of NaOH (15% in water), and 3.3 mL of water were added successively. The solution was filtered, the ether was evaporated, and the residue was distilled. Bp (20 mbar): 75 °C. ^{13}C-NMR (62.90 MHz, $CDCl_3$, 27 °C): δ −2.70 (q, $^{1}J_{CH}$ = 119 Hz, CH_3), 7.02 (t, $^{1}J_{CH}$ = 163 Hz, CH_2 cyclopropane ring), 8.99 (s, quarternary carbon), 70.54 (t, $^{1}J_{CH}$ = 143 Hz, CH_2OH group). ^{1}H-NMR: δ −0.04 (CH_3), 0.26−0.42 (ring CH_2 protons), 3.42 (CH_2OH methylene protons). FT-IR (NaCl, film): 839 (s, ν_{def} cyclopropane ring), 1249 (s, ν_{def} $Si(CH_3)_3$ group), 2955 (s, ν_{sym} CH_2OH methylene C−H bond), 3067 (w, ν_{sym} ring methylene C−H bonds), 3344 (s, ν_{sym} of O−H bond).

(1′-(Trimethylsilyl)cyclopropyl)carbaldehyde (6).[43] A solution of 0.69 mL (7.6 mmol) of oxalyl chloride in 17 mL of CH_2Cl_2 was cooled to −60 °C. Me_2SO (1.17 mL, 15.2 mmol) dissolved in 3.5 mL of CH_2Cl_2 was added. After 2 min, 1.0 g (6.9 mmol) of (1′-(trimethylsilyl)cyclopropyl)methanol (**5**) dissolved in 7 mL of CH_2Cl_2 was added in 5 min and stirring was continued for 15 min. Triethylamine (4.8 mL, 34.5 mmol) was added. The reaction mixture was allowed to warm to room temperature. Stirring was continued for 5 min more, and 34.5 mL of water was added. The aqueous layer was extracted with CH_2Cl_2. The organic layers were combined, washed with brine, and dried over anhydrous $MgSO_4$. Kugelrohr distillation gave a 72% yield of pure (1′-(trimethylsilyl)cyclopropyl)carbaldehyde (**6**). Bp (20 mbar): 55 °C. ^{13}C-NMR (62.90 MHz, $CDCl_3$, 27 °C): δ −3.00 (q, $^{1}J_{CH}$ = 118 Hz, CH_3), 9.58 (t, $^{1}J_{CH}$ = 165 Hz, CH_2 of cyclopropane ring), 20.03 (s, quarternary carbon), 200.69 (d, $^{1}J_{CH}$ = 161 Hz, carbonyl carbon). ^{1}H-NMR: δ 0.03 (CH_3), 0.96/1.05 (ring methylene protons), 8.54 (aldehyde proton). FT-IR (NaCl, film): 843 (s, ν_{def} cyclopropane ring), 1250 (s, ν_{def} $Si(CH_3)_3$ group), 1699 (s, ν_{sym} carbonyl group), 2683 (m, ν_{sym} aldehyde C−H bond), 2957 (s, ν_{sym} methyl C−H bonds), 3078 (w, ν_{sym} methylene C−H bonds).

(1′-(Trimethylsilyl)cyclopropyl-d_1)methanol (5-d_1). A solution of 700 mg (4.9 mmol) of (1′-(trimethylsilyl)cyclopropyl)carbaldehyde (**6**)

(41) Sieber, S.; Otto, A. H.; Schleyer, P. v. R.; Gauss, J.; Reichel, F.; Cremer, D. *J. Phys. Org. Chem.* **1993**, *6*, 445. Sieber, S.; Schleyer, P. v. R.; Gauss, J. *J. Am. Chem. Soc.* **1993**, *115*, 6987. Buzek, P.; Schleyer, P. v. R.; Vancik, H.; Mihalic, Z.; Gauss, J. *Angew. Chem.* **1994**, *104*, 470. Siehl, H.-U.; Müller, T.; Gauss, J.; Buzek, P.; Schleyer, P. v. R. *J. Am. Chem. Soc.* **1994**, *116*, 6384.

(42) Warner, P. M.; Le, D. *J. Org. Chem.* **1982**, *47*, 893.

(43) Mancuso, A. J.; Huang, S.-L.; Swern, D. *J. Org. Chem.* **1978**, *43*, 2480.

in 10 mL of dry ether was added to a stirred suspension of 1.0 g (23.9 mmol) of lithium aluminium deuteride in 20 mL of dry ether, and the resulting mixture was stirred for 3 h. After usual workup the product was purified by distillation. Bp (20 mbar): 75 °C. ^{13}C-NMR (62.90 MHz, $CDCl_3$, 27 °C): δ −2.70 (q, $^1J_{CH}$ = 119 Hz, CH_3), 7.02 (t, $^1J_{CH}$ = 163 Hz, CH_2 cyclopropane ring), 8.99 (s, quarternary carbon), 70.30 (t of d, $^1J_{CH}$ = 143 Hz, $^1J_{CD}$ = 22 Hz, CHDOH group). ^{1}H-NMR: δ −0.02 (CH_3), 0.26−0.42 (ring methylene protons), 3.42 (t, $^1J_{HD}$ = 2 Hz, CHDOH methylene proton). FT-IR (NaCl, film): 837 (s, ν_{def} cyclopropane ring), 1252 (s, ν_{def} $Si(CH_3)_3$ group), 2141 (m, ν_{sym} C−D bond), 2955 (s, ν_{sym} of CHDOH methylene C−H bond), 3067 (w, ν_{sym} ring methylene C−H bonds), 3324 (s, ν_{sym} of O−H bond).

(1′-(Trimethylsilyl)cyclopropyl-d_2)methanol (5-d_2). A solution of 2.5 g (0.016 mol) of (1′-(trimethylsilyl)cyclopropyl)carboxylic acid (**7**) in 20 mL of dry ether was added to a stirred suspension of 1.0 g (0.024 mol) of lithium aluminium deuteride in 30 mL of dry ether, and the resulting mixture was stirred for 3 h. Usual workup yielded **5**-d_2. Bp (20 mbar): 75 °C. ^{13}C-NMR (62.90 MHz, $CDCl_3$, 27 °C): δ −2.67 (q, $^1J_{CH}$ = 119 Hz, CH_3), 7.03 (t, $^1J_{CH}$ = 163 Hz, CH_2 cyclopropane ring), 8.92 (s, quarternary carbon), 69.95 (quintet, $^1J_{CD}$ = 26 Hz, CD_2-OH group). ^{1}H-NMR: δ −0.02 (CH_3), 0.28−0.45 (ring methylene protons). FT-IR (NaCl, film): 839 (s, ν_{def} cyclopropane ring), 1254 (s, ν_{def} $Si(CH_3)_3$ group), 2183 and 2081 (m, ν_{sym} C−D bonds), 2955 (s, ν_{sym} methyl C−H bonds), 3067 (w, ν_{sym} ring methylene C−H bonds), 3344 (s, ν_{sym} of O−H bond).

Preparation of the Carbocations. The general experimental technique and the special apparatus for the generation of carbocations has been described.[44] At a pressure of 10^{-5} mbar, 0.5 mmol of the precursor alcohol and 0.6 mL of SbF_5 were distilled synchronously through separate nozzles onto a homogeneous matrix of 0.7 mL of SO_2F_2, 1.4 mL of SO_2ClF, and 10 mg of tetramethylammonium tetrafluoroborate (TMA) cooled to −196 °C. After completion of the co-condensation another 0.7 mL of SO_2F_2 and 1.4 mL of SO_2ClF were condensed onto the matrix. A lightly yellow solution of **3** was obtained by warming to −135 °C. The solution was transferred under high vacuum at −135 °C into 10 mm NMR tubes, which were then sealed under vacuum and stored at −196 °C.

^{1}H-NMR and ^{13}C-NMR spectra of the carbocation solutions are measured on a Bruker AMX 400 NMR spectrometer equipped with a variable-frequency fluorine lock channel and a 10 mm ^{13}C/^{1}H/^{19}F probe, using the fluorine resonance of SO_2ClF or SO_2F_2 as an internal lock. TMA ($Me_4N^+BF_4^-$) was used as internal standard (^{1}H-NMR: δ = 3.0 ppm; ^{13}C-NMR: δ = 55.65 ppm). The probe temperature was calibrated with a ^{13}C chemical shift thermometer using neat 2-chlorobutane[45] in a capillary in an NMR tube filled with SO_2ClF admixed with other solvents.

Quantum chemical calculations of structures and energies were done at Tübingen on the Convex C3860 computer of the computer center at the University of Tübingen using the Gaussian 90 and 92 program suite and on SGI INDIGO and INDY workstations using the Gaussian 92 program.[33] The GIAO calculations were done at Karlsruhe on IBM RS6000 workstations and at Tübingen on SGI workstations using the ACES II program.[39]

Acknowledgment. The work at Tübingen was supported by the Deutsche Forschungsgemeinschaft. Thanks go to the Japanese Society for the Promotion of Science for support of a visiting professorship of H.-U.S. at Kyushu University and the Fonds der Chemischen Industrie. We thank R. Ahlrichs, Karlsruhe, and Y. Tsuno, Kyushu University, Japan, for support.

JA950644K

(44) Lenoir, D.; Siehl, H.-U. In *Houben-Weyl Methoden der Organischen Chemie*; Hanack, M., Ed.; Thieme: Stuttgart, Germany, 1990; Vol. E19c, pp 26−32.

(45) Schneider, H.- J.; Freitag, W. *J. Am. Chem. Soc.* **1976**, *98*, 478.